Research Article

Comparisons of Performances between the Single-Pass and Double-Pass Hybrid Photovoltaic/Thermal (PV/T) Air Heating Collector by Using Mathematical Models

Yod Sukamongkol*
Energy Engineering Program, Faculty of Engineering, Ramkhamhaeng University, Ramkhamheang Rd., Huamark, Bangkapi, Bangkok 10240, Thailand

Abstract

The hybrid photovoltaic/thermal (PV/T) air heating collector consists of a conventional photovoltaic (PV) module and an attached air flow channel with internal working fluid flowing to extract thermal energy from the PV module; therefore, the electrical efficiency of the PV module can be increased by reducing its operating temperature. This paper presents the comparison results of the predicted performances of single-pass and double-pass PV/T air heating collectors by using the developed simulation models. Three types of PV/T collectors are considered: type A (the air flow channel is above the PV modules), type B (the air flow channel is under the PV modules) and type C (the air flow channels are above and under the PV modules). Based on energy-balance equations, the mathematical models for each component in the PV/T collector, such as glass cover, air flow channel, PV/T absorber and back metal plate, have been developed. Using the same meteorological data input, the simulated results indicate that the maximum electrical efficiencies of collectors type A, B and C are 4.6%, 5.2%, and 5.0%, respectively, while the thermal efficiencies of these collectors are up to 39%, 46%, and 59%, respectively. It is obvious from the results that the configurations in the PV/T air heating collector have influences on their electrical and thermal performances.

Keywords: Hybrid Photovoltaic/Thermal; Air Heating Collector; Simulation model; Conversion Efficiency

1. Introduction

Solar energy is mainly utilized in two categories – thermal energy and electrical energy. Those energies are generally generated separately by two systems which are solar heating system and photovoltaic system, respectively. The efficiency of solar heating collectors is higher than 50% [1], while that of solar cells is about 15% and generally temperature-dependent, usually decreasing as the temperature increases [2,3]. By proper circulation of a fluid with low inlet temperature, heat is extracted from the solar cell module; therefore, its efficiency is increased. As a result, this heat can be harnessed by combining both the thermal system and photovoltaic system in a hybrid photovoltaic/thermal (PV/T) energy system.

***Correspondence** : yod_skm@yahoo.com DOI 10.14456/tijsat.2016.5

A hybrid PV/T air heating collector is basically constructed by pasting solar cells directly over the absorber plate of the solar collector; thus, it can simultaneously produce the two types of energies required by most consumers: low temperature heat and electricity. The solar energy from the sun is partly converted to electricity by photovoltaic cells in thermal contact with a solar heat absorber so that the excess heat generated in the photovoltaic cells can be used as input for the thermal system. During operation, a heat carrier fluid removes heat from the absorber and the solar cells so that they operate at a low and stable temperature which increases the electrical power output of the solar cell [4,5].

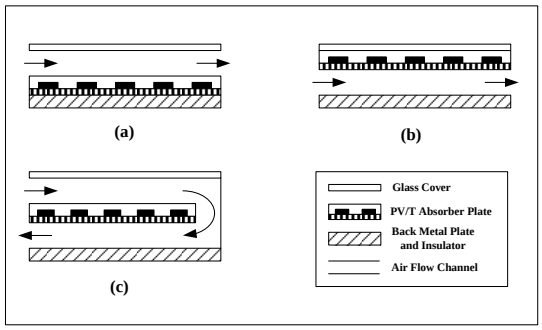

Fig.1. Physical Configurations of PV/T Air Heating Collectors.

The photovoltaic panel used in a PV/T air heating collector could be the mono-crystalline, poly-crystalline, amorphous silicon or thin-film solar cell, while there are some designs of solar thermal collectors which extract heat from the PV panel [6, 7]. The cross sectional views of the various PV/T air heating collectors are shown in Figure 1. Figure 1(a) presents the physical configuration of the single-pass PV/T air heating collector Type A which consists of four significant components: a glass cover (g), upper air flow channel (f1), a PV/T absorber plate (p) and a back metal plate (b). The ambient air enters the PV/T collector at the upper flow channel, which is formed between the glass cover and the front side of the PV/T absorber plate. Next, the physical configuration of the four components of the single-pass PV/T air heating collector Type B is illustrated in Figure 1(b). It is almost the same as that of Type A except the under flow channel (f2), which is formed between the back side of the PV/T absorber plate and the back metal plate [8,9].

For the double-pass PV/T air heating collector, its basic physical configuration used in this study is shown in Figure 1(c). The model is composed of five significant components that are: a glass cover, upper Flow Channel 1, a PV/T absorber plate, under Flow Channel 2, and a back metal plate. The ambient air is drawn to enter the collector for the first pass through the upper Flow Channel 1 where a part of solar energy absorbed by the PV/T absorber plate is transferred to the passing air. At the end of the channel, the warm air is drawn down to enter the under Flow Channel 2. In this second pass, the warm air is further heated up by another part of the heat in the PV/T absorber plate which leaves the collector at the bottom side of the plate. This flow arrangement results in greater heat removal from the PV/T absorber and leads to higher temperature of the air flowing out at the collector outlet. The solar cells on the PV/T absorber plate, once again cooled by the heat carrier, give increased solar cell efficiency output [10,11,12].

The objective of this paper is to develop the simulation models of each component of PV/T air heating collectors (Type A, B and C) based on energy balance equations for predicting their performances. The simulations are run under the same prevailing meteorological and operating conditions in a tropical climate. Then, the simulated results are compared and presented.

2. Simulation Model

2.1 Simulation Model of PV/T Air Heating Collector with various Types

Various assumptions are made in order to simplify the thermal analysis of the PV/T air heating collector based on its

components. They can be explained as follows:

1) It is assumed that the heat distribution in every component is uniform, therefore the heat capacitance of the component is lumped and its temperature represented as the effective temperature.
2) Thermal and optical properties (i.e. absorptivity, emissivity, transmittivity, thermal conductivity and specific heat coefficient) of all components (i.e. glass cover, PV/T absorber plate, back metal plate, insulation and process air) are constant and not a function of temperature.
3) The heat capacity of the metal casing of the collector is very small and negligible in comparison with those of other components.
4) As the thickness of the collector is relatively small compared to its length and width, it is assumed that the heat losses at the sides and the edge of the collector are small and negligible.
5) The air mass flow rate is assumed to be uniform throughout the PV/T collector.
6) The type of PV module used in the study is the 42-W_p amorphous-silicon (a-Si) thin-film solar cell module.

Therefore, the mathematical models based on energy balance equations for difference components can be expressed as

Type A: A single-pass PV/T air heating collector which has an air flow channel over the photovoltaic panel.

For Glass Cover (*g*),

$$m_g C_g (dT_g/dt) = \alpha_g G A_g - A_g F_{g\to sky}\sigma(\varepsilon_g T_g^4 - \varepsilon_{sky} T_{sky}^4) - A_g h_{c,g\to a}(T_g - T_a) - A_g h_{c,g\to f1}(T_g - T_{f1}) + A_g h_{r,p\to g}(T_p - T_g) \quad (1)$$

For Air Flowing in upper Channel (*f1*),

$$m_a C_a (dT_{f1}/dt) = A_g h_{c,g\to f1}(T_g - T_{f1}) + A_p h_{c,p\to f1}(T_p - T_{f1}) - \dot{m}_{a,PV/T} C_a (T_{f1out} - T_{f1in}) \quad (2)$$

For PV/T Absorber (*p*),

$$(m_p C_p)(dT_p/dt) = \alpha_S \tau_g G A_p - A_p h_{r,p\to g}(T_p - T_g) - A_p h_{c,p\to f1}(T_p - T_{f1}) - A_p h_{r,p\to b}(T_p - T_b) - \eta_S \tau_g G A_p \quad (3)$$

For Back Metal Plate (b),

$$m_b C_b (dT_b/dt) = A_p h_{r,p\to b}(T_p - T_b) - A_b U_{ba}(T_b - T_a) \quad (4)$$

Type B: A single-pass PV/T air heating collector which has an air flow channel under the photovoltaic panel.

For Glass Cover (*g*),

$$m_g C_g (dT_g/dt) = \alpha_g G A_g - A_g F_{g\to sky}\sigma(\varepsilon_g T_g^4 - \varepsilon_{sky} T_{sky}^4) - A_g h_{c,g\to a}(T_g - T_a) + A_g h_{r,p\to g}(T_p - T_g) \quad (5)$$

For PV/T Absorber (*p*),

$$(m_p C_p)(dT_p/dt) = \alpha_S \tau_g G A_p - A_p h_{r,p\to g}(T_p - T_g) - A_p h_{c,g\to f2}(T_p - T_{f2}) - A_p h_{r,p\to b}(T_p - T_b) - \eta_S \tau_g G A_p \quad (6)$$

For Air Flowing in under Flow Channel (*f2*),

$$m_a C_a (dT_{f2}/dt) = A_p h_{c,p\to f2}(T_p - T_{f2}) + A_b h_{c,b\to f2}(T_b - T_{f2}) - \dot{m}_{a,PV/T} C_a (T_{f2out} - T_{f2in}) \quad (7)$$

For Back Metal Plate (b),

$$m_b C_b (dT_b/dt) = A_p h_{r,p\to b}(T_p - T_b) - A_b h_{c,b\to f2}(T_b - T_{f2}) - A_b U_{ba}(T_b - T_a) \quad (8)$$

Type C: A double-pass PV/T air heating collector which has air flow channels over and under the photovoltaic panel [13].

For Glass Cover (*g*),

$$m_g C_g (dT_g/dt) = \alpha_g G A_g - A_g F_{g\to sky}\sigma(\varepsilon_g T_g^4 - \varepsilon_{sky} T_{sky}^4) - A_g h_{c,g\to a}(T_g - T_a) - A_g h_{c,g\to f1}(T_g - T_{f1}) + A_g h_{r,p\to g}(T_p - T_g) \quad (9)$$

For Air Flowing in upper Flow Channel (*f1*),

$$m_a C_a (dT_{f1}/dt) = A_g h_{c,g\to f1}(T_g - T_{f1}) + A_p h_{c,p\to f1}(T_p - T_{f1}) - \dot{m}_{a,PV/T} C_a (T_{f1out} - T_{f1in}) \quad (10)$$

For PV/T Absorber (*p*),

$$(m_p C_p)(dT_p/dt) = \alpha_S \tau_g G A_p - A_p h_{r,p\to g}(T_p - T_g) - A_p h_{c,p\to f1}(T_p - T_{f1}) - A_p h_{c,g\to f2}(T_p - T_{f2}) - A_p h_{r,p\to b}(T_p - T_b) - \eta_S \tau_g G A_p \quad (11)$$

For Air Flowing in under Flow Channel (*f2*),

$$m_a C_a (dT_{f2}/dt) = A_p h_{c,p\to f2}(T_p - T_{f2}) - A_b h_{c,b\to f2}(T_b - T_{f2}) - \dot{m}_{a,PV/T} C_a (T_{f2out} - T_{f2in}) \quad (12)$$

For Back Metal Plate (b),

$$m_b C_b (dT_b/dt) = A_p h_{r,p\to b}(T_p - T_b) - A_b h_{c,b\to f2}(T_b - T_{f2}) - A_b U_{ba}(T_b - T_a) \quad (13)$$

2.2 Determination of Parameters used in Simulation Model

The sky temperature is assumed to be close to the ambient temperature as [14]:

$$T_{sky} \approx 0.914 T_a . \quad (14)$$

As the back metal plate and collector casing are thin, the overall heat loss coefficient from back plate to ambient air U_{ba} can be approximately determined from:

$$U_{ba} = \left[1/\left(L_{ins}/k_{ins}\right)\right] \quad (15)$$

The convective heat transfer coefficient from the glass cover to the ambient air for panel tilted at an angle β below 25° and for low moderate wind speed, V_{wind}, is expressed as:

$$h_{cga} = 1.2475\left[\left(T_g - T_a\right)\cos\beta\right]^{0.33} + 2.685 V_{wind} \quad (16)$$

The forced convective heat transfer coefficient, h_c, of air flowing between any parallel flat plates with spacing, D, can be found by using the dimensionless quantities [14] which are Nusselt number (N_u) and Reynolds number (R_e) as follows:

$R_e = (\rho V D)/\mu$, $N_u = 0.0158 R_e^{0.8}$, and $h_c = (N_u k)/D$ (17)

The radiative heat transfer coefficient, h_r, between any two surfaces 1 and 2 can be determined by

$$h_r = 4\sigma \bar{T}^3 / \left(1/\varepsilon_1 + 1/\varepsilon_2 - 1\right) \quad (18)$$

Last, the average daily PV/T collector efficiency can be can be expressed as [13, 15]:

$$\eta_{PV/T} = \eta_{th} + \eta_S = \left(\int Q_{th} dt + \int P_{elec} dt\right) / \left(A_g \int G dt\right) \quad (19)$$

where $Q_{th} = m_a C_a (T_{fout} - T_{fin})$, $P_{elec} = \eta_S \tau_g G A_p$.

and $\eta_S = \eta_{ref}[1 - \gamma(T_p - T_{ref})]$ (20)

3. Configuration of Simulation Model

The simulation models, consisting of the mathematical equations of all the components of these three types of PV/T air heating collectors, are developed and calculated using MATLAB. These simulation models have been carried out for the hybrid PV/T solar air heating collectors consisting of a 2-m^2 single-glass collector with single-pass and double-pass air flow channels as described above with three 42-Wp amorphous-silicon (a-Si) thin-film solar cell modules pasting over an aluminum absorber plate. The other designed parameter values of PV/T collectors are presented in Table 1.

The system was assumed to be operated under the typical climate conditions of Bangkok located at the latitude 14°N. The total solar irradiance, ambient temperature and wind speed were measured by a pyranometer, a digital thermometer with thermocouple type K and an anemometer, respectively. These data were recorded by a data-logger every minute and the average values of every hour were stored. These meteorological data were used as the inputs of the simulation models.

Table 1. The parameters of designed PV/T air heating collectors.

Parameters	Values	Unit	Remarks	Parameters	Values	Unit	Remarks
Dimension	(W x L x Thickness)		Fixed	Specific heat C_g	837	J/kgK	Standard Values at 25°C
Glass Cover	0.95 x 2.35 x 0.004	m^3		C_f	1.007	J/kgK	
PV/T Absorber Plate	0.95 x 2.15 x 0.003	m^3		C_b	903	J/kgK	
Back Metal Plate	0.95 x 2.35 x 0.001	m^3		Emissivity ε_g	0.88		
Insulator	0.95 x 2.35 x 0.040	m^3		ε_p	0.82		
Density ρ_g	2515	kg/ m^3	Standard Values at 25°C	Viscosity, μ_a	1.562×10^{-5}	m^2/s	
ρ_f	1.184	kg/ m^3					
ρ_b	7,870	kg/ m^3		Overall heat loss coefficient U_{tb}	0.9	W/m^2K	From Manufacturer's Data
Mass m_g	22.458	kg	Calculated from	Efficiency of solar cell at reference temperature, η_r	6.5	%	
m_f	0.261	kg		Temperature coefficient of solar cell, γ	0.0015	K^{-1}	
m_b	24.382	kg	$m = \rho V$	Effective Thermal capacity, $m_g C_g$	9,950	J/K	
Mass flow rate of air	0.05	kg/s	Fixed	Overall absorbtivity of PV/T absorber plate	0.816		

4. Results and Discussions

The prevailing variations of the solar irradiance, ambient temperature, and wind speed of the observed day are shown in Figure 2. The irradiance rose up to 970 W/m^2 at noon while the ambient temperatures were around 25 ºC during the night and increased to 35 ºC in the daytime. The wind speed was in the range between 0.5 - 3 m/s.

Figure 3 presents the variations of PV/T absorber temperatures which were initially set to be equal to the ambient condition. The overall variation trends of all types were similar. In the morning, the PV/T collector was heated up by solar irradiance and a rise in ambient temperature, while it declined in the afternoon. The maximum temperature of Type A was 80ºC while those of Type B and C were lower, 66 ºC and 71 ºC, respectively. It can be explained that the air flowing over the solar cell weakens heat extraction, and on the other hand, the air flowing under the solar cell gains more heat extraction.

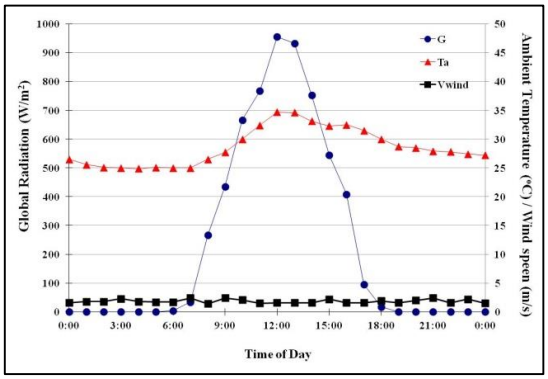

Fig.2. Hourly Solar Radiation, Ambient Temperature and Wind Speed Input Data**.**

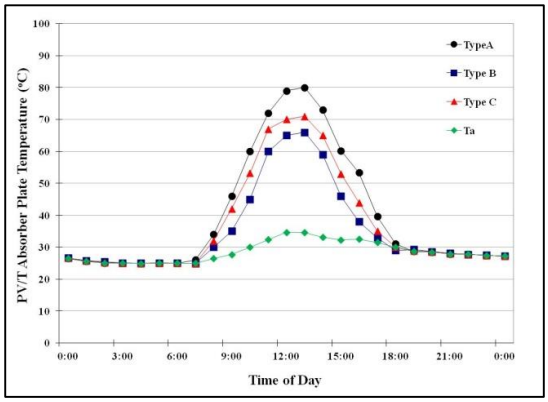

Fig.3. Hourly Variations of PV/T Absorber Plate Temperature**.**

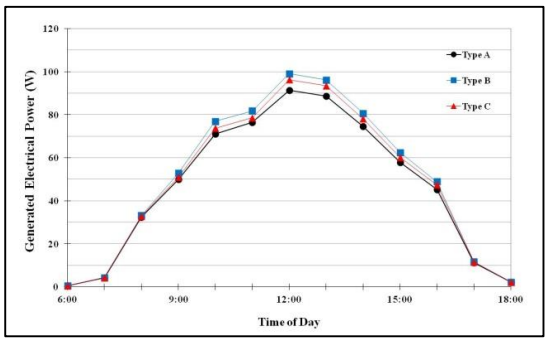

Fig.4. Hourly Variations of Generated Electrical Power**.**

The hourly variation of generated electrical power is illustrated in Figure 4. Due to the same solar irradiance input, the generated power of Type A, B and C were 90, 100 and 96W, respectively. It is obviously seen that Type B could generate more electrical power than Type A and C. This resulted from the fact that there was a negative correlation between the PV generated electrical power output and PV cell temperature. Therefore, the higher PV/T temperatures shown in Figure 3 lead to the lower power generation shown in Figure 4. These results are similar to those studied by Sukamongkol *et- al.* [15]. Moreover, these results are consequences to the electrical efficiency that is defined as a ratio of generated electrical power to the solar radiation power received by PV/T air heating collector. Figure 5 shows the hourly variation

of simulated electrical efficiency. Based on the specification of a-Si thin-film solar cell modules used in the study, the initial electrical efficiency was 6.5%. With the same solar power input, the lower generated power resulted in the lower conversion efficiency. Thus, the minimum electrical efficiencies of Type A, B and C are 4.6%, 5.2% and 5.0%, respectively. It can be concluded that the electrical performances of Type B are optimal.

Figure 6 presents the variation of the temperature of air flowing out from the PV/T air heating collector. Starting with the same value as ambient temperature, the air temperatures increased in the morning and decreased in the afternoon with the same trend as that of PV/T absorber temperature. The air temperature output of Type C was the highest (52^{o}C) because the working air passed through the upper and under flow channel (double-pass), where it was heated in channel 1 (between the glass cover and PV/T absorber plate) and channel 2 (between the PV/T plate and the back plate). Comparison of Type A and B showed that their peak temperature outputs were about 44 ^{o}C and 48 ^{o}C which indicated that air flowing under the PV/T absorber enhanced more heat extraction. These results agree with those observed by Sopian *et- al.* [12] and Sukamongkol *et- al.* [13].

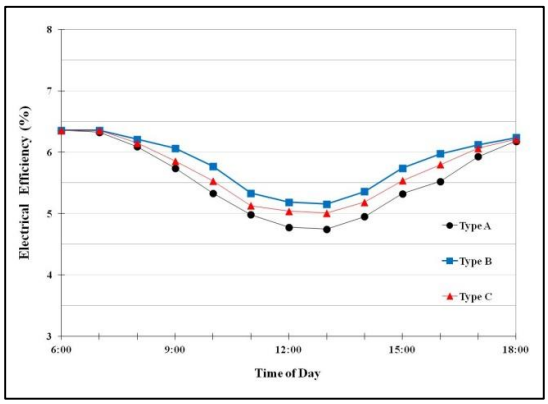

Fig.5. Hourly Variations of Simulated Electrical Efficiency.

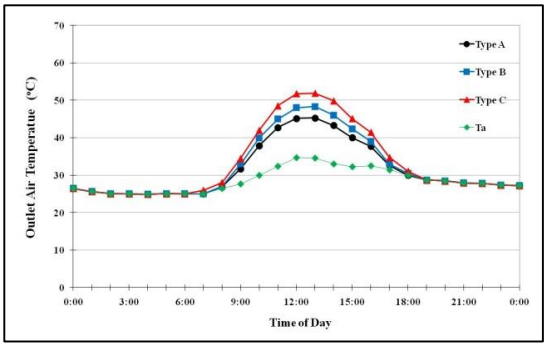

Fig.6. Hourly Variation of Heated Air Output Temperature.

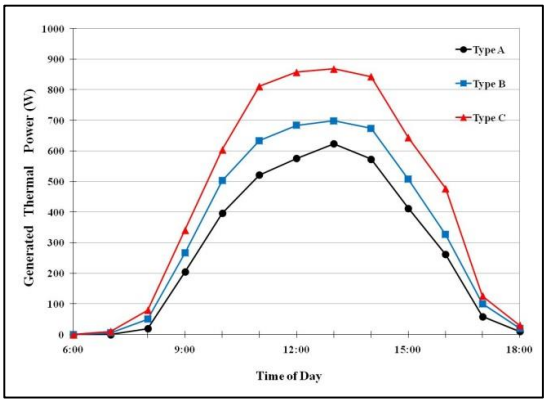

Fig.7. Hourly Variation of Generated Thermal Power.

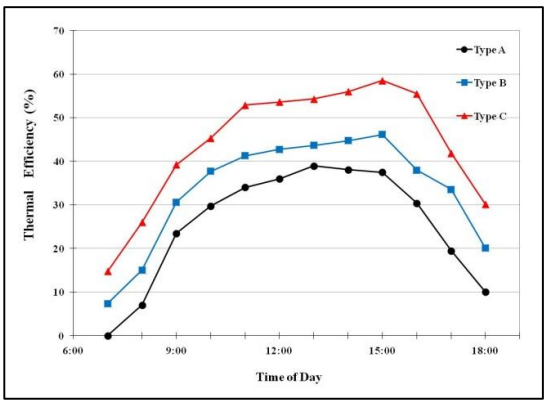

Fig.8. Hourly Variation of Simulated Thermal Efficiency.

The hourly variation of generated thermal power is presented in Figure 7. According to eq.(20), the higher air output temperatures result in the higher thermal power output. Therefore, Type C generated the highest

thermal power output of 880 W, while those of Type A and B were 610 and 700 W, respectively. Figure 8 shows the hourly variation of thermal efficiency, which is described as a ratio of thermal power output to the solar radiation power input. It was clearly seen that the thermal efficiencies of Type A, B and C were high, up to 39%, 46% and 59%, respectively. Thus, it can be concluded that the thermal performance of Type C is optimal.

In addition, the variations of total conversion efficiencies of the three types of PV/T air heating collectors were shown in figure 9. The highest values of overall efficiency of Type A, B and C are 44%, 51% and 65%, respectively.

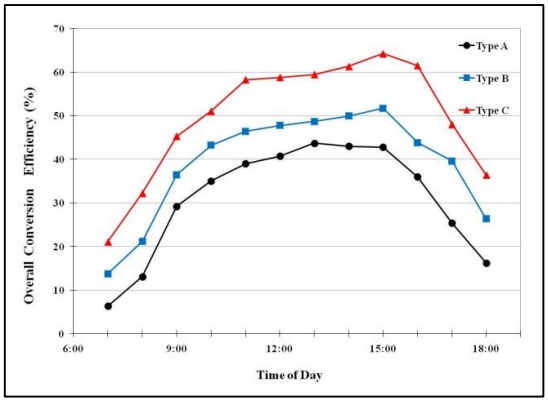

Fig.9. Hourly Variation of Overall Thermal Efficiency.

5. Conclusions

It can be concluded from the simulated validation results that the developed simulation model was able to predict the performance of the hybrid photovoltaic/thermal air heating collectors, both single-pass and double-pass types. For the electrical performances, the generated electrical power rose along with the increment of solar radiation intensity but their electrical efficiency decreased, resulting from the rise of PV cell temperature. Next, the generated thermal power and the heated air output temperature were also increased with the increment of solar radiation intensity. In addition, the maximum simulated overall efficiency of the double-pass PV/T air heating collector (Type C) was 65% which was more than the 44% and 51% of the single-pass collectors Types A and B, respectively. Although the models can predict the results of interest, these simulation models should be verified by the various experiments. However, the configurations of PV/T air heating collectors should be optimized according to the specific priority needs, such as generated electrical power, generated thermal power or the heated air output temperature. Besides, the feasibility resulting from the different configurations of PV/T collectors and types of PV module should be taken into account for further works.

6. Nomenclature

A = Area (m^2), C = Specific heat (J/kg K), COP = Coefficient of performance, , D_h = Hydraulic diameter of air flow channel (m), F = View Factor, G = Solar Irradiance (W/m^2), h = Heat Transfer Coefficient (W/m^2K), m = Mass (kg), $\dot{m}$ = Mass flow rate (kg/s), n = infiltration rate (%), P = Pressure (Pa), P_{elec} = Electrical power (W), Q = amount of thermal energy (MJ), T = Temperature (K), t = Time (s), and U = Overall heat loss coefficient (W/m^2K).

Greek letters: α = absorptance, σ = Stephan-Boltzmann constant, τ = transmittance, η= efficiency, ε = emissivity, and h = enthalpy.

Subscripts: a = ambient, b = back plate, c or $conv$ = convective, con = condenser, $elec$ = electrical, $f1$ = working fluid (air) at upper channel, $f2$ = working fluid (air) at under channel, g = glass cover, in = input, ins = insulation, out = output, p = PV/T absorber plate, rad = radiative, sky = sky, th = thermal, u = useful energy, and $\rightarrow$ = to.

7. References

[1] Goswami, D. Y., Kreith, F. and Kreider, J. F., *Principles of Solar Engineering*, George H. Buchanan Co 2nd Ed., PA, USA., 1999.

[2] Green, M. A., *Solar Cells: Operating Principles, Technology, and System*

Application, Prentice-Hall, USA., 1985.

[3] Messenger, R.A. and Ventre, J., Photovoltaic System Engineering, *CRC*, 2004.

[4] Cox, C.H., III and Raghuraman, P., Design Considerations for Flat-Plate Photovoltaic/ Thermal Collectors, *Solar Energy*, Vol.35, No.3, pp. 227-241, 1985.

[5] Lalavic, B., A Hybrid Amorphous Silicon Photovoltaic and Thermal Solar Collector, *Solar cells*, Vol.19, pp. 131-138, 1987.

[6] Garg H.P. and Adhikari, R. S., Conventional Hybrid Photovoltaic/Thermal (PV/T) Air Heating Collectors: Steady-state Simulation, *Renewable Energy*, Vol. 11, No.3, pp.363-385, 1997.

[7] Garg, H.P. and Adhikari, R.S., System Performance Studies on a Photovoltaic/ Thermal (PV/T) Air Heating Collector, *Renewable Energy*, Vol.16, pp.725-730, 1999.

[8] Kalogirou, S.A. and Tripanagnostopoulos, Y., Photovoltaic Thermal (PV/T) Collectors: A Review, *Applied Thermal Engineering*, Vol. 27, Issues 2-3, pp. 275-286, 2007.

[9] Sopian, K., Yigit, K.S., Liu, H.T., Kakac, S. and Verziroglu, T.N., Performance Analysis of Photovoltaic Thermal Air Heaters, *Energy Conversion and Management*, Vol.37, No.11, pp.1657-1670, 1996.

[10] Chow T.T., A Review on Photovoltaic/ Thermal Hybrid Solar Technology. Apply Energy, Vol.87, pp.365-79, 2010.

[11] Sukamongkol, Y., Chungpaibulpatana, S., Limeechokchai, B. and Sripadungtham, P., Simulation of a Hybrid Photovoltaic-Thermal (PV-Th) Air Heating System for Regenerating Desiccant Gel in an Air Conditioning Room, Asian Journal of Energy & Environment, Vol.9, pp.129-160, 2008.

[12] Sopian, K., Liu, H.T., Kakac, S. and Veziroglu, T.N., Performance of a Double Pass Photovoltaic Thermal Solar Collector Suitable for Solar Drying System, *Energy Conversion and Management*, Vol.41, pp.353-365, 2000.

[13] Sukamongkol, Y., Chungpaibulpatana, S., Limmeechokchai, B. and Sripadungtham, P., Condenser Heat Recovery with a Solar Air Heating Collector to Regenerate Desiccant for Reducing Energy Consumption of an Air Conditioning Room, *Energy and Buildings*, Vol.42, No.3, pp. 315-325, 2010.

[14] Duffie, J.A. and Beckman, W.A., Solar Engineering of Thermal Processes, *John Wiley & Sons*, 4nd Ed., USA, 2013

[15] Sukamongkol, Y., Chungpaibulpatana, S. and Ongsakul, W., A Simulation Model for Predicting the Performance of a Solar Photovoltaic System with Alternating Current Loads, *Renewable Energy*, Vol.27, pp. 237-258, 2002